DR PETER T PELLITIER (Orcid ID : 0000-0002-0226-0784)
DR DONALD R ZAK (Orcid ID : 0000-0002-9730-7337)

Article type : MS - Regular Manuscript

Ectomycorrhizal fungal decay traits along a soil nitrogen gradient

Peter T. Pellitier[1*] & Donald R. Zak[1,2]

[1]School for Environment and Sustainability, University of Michigan. Ann Arbor, Michigan, USA 48109; [2]Department of Ecology and Evolutionary Biology, University of Michigan. Ann Arbor, Michigan, USA 48109. Orchid IDs : Peter T. Pellitier: 0000-0002-0226-0784; Donald R. Zak: 0000-0002-9730-7337

Author for Correspondence:
Peter T. Pellitier
Department of Biology, Stanford University, Stanford California USA.
Email: ptpell@stanford.edu;
Tel: +1 541-554-4706

Received: 18 May 2021
Accepted: 16 August 2021

Summary:

- The extent to which ectomycorrhizal fungi decay soil organic matter SOM has implications for accurate predictions of forest ecosystem response to climate change. The

distribution of gene-traits associated with SOM decay remains poorly understood among ectomycorrhizal fungal communities. We hypothesized that soil inorganic N availability acts as an environmental filter that structures the distribution of genes associated with SOM decay and specifically, that ectomycorrhizal fungal communities occurring in inorganic N poor soils have greater SOM decay potential.

- To test this hypothesis, we paired amplicon and shotgun metagenomic sequencing of 60 ectomycorrhizal fungal communities associating with *Quercus rubra* L. along a natural soil inorganic N gradient.
- Ectomycorrhizal fungal communities occurring in low inorganic N soils were enriched in gene families involved in the decay of lignin, cellulose, and chitin. Ectomycorrhizal fungal community composition were the strongest driver of shifts in metagenomic estimates of fungal decay potential. Our study illuminates the identity of key ectomycorrhizal fungal taxa and gene families potentially involved in the decay of SOM, and we link rhizomorphic and medium-distance hyphal morphologies with enhanced SOM decay potential.
- Coupled shifts in ectomycorrhizal fungal community composition and community level decay gene frequencies are consistent with outcomes of trait-mediated community assembly processes.

Keywords: community aggregated traits, community assembly, Ectomycorrhizal fungi, organic nitrogen, shotgun metagenomics, soil gradient, soil organic matter

Introduction:

Understanding microbial community assembly and function (Nemergut *et al.*, 2013) is critical to the incorporation of microbial processes into biogeochemical models (Hall *et al.*, 2018; Fry *et*

al., 2019; Bradford *et al.*, 2021). Trait-based frameworks developed for plant ecology (Diaz *et al.*, 1998; Cornwell & Ackerly, 2009) can be applied to investigate microbial community assembly (Fierer *et al.*, 2014; Malik *et al.*, 2020a). For example, plant traits subject to environmental filtering have been inferred by analyzing community-level trait distributions along abiotic gradients (Cornwell & Ackerly, 2009; Bernard-Verdier *et al.*, 2012). Functional trait trade-offs may constrain the attributes of viable life-history strategies present in individual taxa. Environmental filters may act on this variation leading to convergent or 'underdispersed' local trait distributions and significant associations between environmental conditions and species functional traits (Diaz *et al.*, 1998; Ackerly & Cornwell, 2007). While trait trade-offs are increasingly characterized for a wide range of microbial taxa (Zanne *et al.*, 2020; Malik *et al.*, 2020a,b), there remains minimal understanding of the role of functional traits in structuring microbial community assembly (Rath *et al.*, 2019; Maynard *et al.*, 2019; Bouma-Gregson *et al.*, 2019).

Microbial communities, especially root mutualists, serve to modify root function and plant fitness across environmental conditions (Peay, 2016; Fitzpatrick *et al.*, 2018; Ravanbakhsh *et al.*, 2019). Ectomycorrhizal (ECM) fungi, in particular, dominate boreal and temperate forest soil microbial communities, providing plant hosts with the majority of their annual nitrogen (N) requirements (~70%) (Smith & Read, 2010). Despite being one of the most studied microbial groups, controls on the distribution of ECM fungal traits remain poorly understood (Courty *et al.*, 2016; van der Linde *et al.*, 2018; Meeds *et al.*, 2021). One prominent ECM fungal functional trait is the acquisition of N bound in soil organic matter (N-SOM), which constitutes the majority of soil N (Vitousek & Howarth, 1991). ECM fungal access to and assimilation of N-SOM is contingent upon the decay of plant and microbially derived compounds present in SOM (Lindahl & Tunlid, 2015; Zak *et al.*, 2019b; Lehmann *et al.*, 2020). Historically only inorganic N and certain simple organic N sources were considered accessible to plants (Schimel & Bennett, 2004); however, recent studies suggest that certain ECM fungi may allow plants to acquire N-SOM and 'short-circuit' limiting supply rates of inorganic N (Lindahl & Tunlid, 2015; Zak *et al.*, 2019b). ECM fungal decay capacity has profound implications for ecosystem function. For example, plant acquisition of N-SOM is one of the most sensitive parameters determining global forest productivity responses to elevated CO_2 (eCO_2) (Terrer *et al.*, 2016, 2021), and ECM fungal decay physiology may impact SOM dynamics at global scales (Orwin *et al.*, 2011; Averill

et al., 2014; Sulman *et al.*, 2019). Despite these emergent findings, factors controlling SOM decay capacity in ECM fungal communities remains poorly understood.

Studies at local, regional and continental scales consistently identify soil inorganic nitrogen (N) availability as a key determinant of ECM fungal community composition (Taylor *et al.*, 2000; Lilleskov *et al.*, 2002a; Peay *et al.*, 2015; van der Linde *et al.*, 2018). Biological market perspectives provide insight into how N availability and fungal N acquisition traits may interact to structure these communities (Koide *et al.*, 2014; Christian & Bever, 2018). Plants may partner with fungal mutualists that maximize N (or P) acquisition, while minimizing photosynthate expenditure (Hortal *et al.*, 2017; Bogar *et al.*, 2019; Meeds *et al.*, 2021). Comparative genomic analyses suggest that ECM fungal decay potential varies widely across the ~ 80 independent evolutionary originations of the ECM fungal lifestyle (Kohler *et al.*, 2015; Shah *et al.*, 2016; Pellitier & Zak, 2018). Accordingly, if the metabolic cost of SOM decay and N-SOM acquisition is high relative to inorganic N acquisition (Hammel & Cullen, 2008; Janusz *et al.*, 2017), ECM fungi with greater SOM decay capacity may be disfavored under certain environmental contexts (Koide *et al.*, 2014). In this study we investigate the outcome of trait-mediated assembly processes that structure the distribution of ECM fungal SOM decay traits and ECM fungal communities along a natural soil inorganic N gradient. We specifically predict that ECM fungal communities occurring in low inorganic N soils are compositionally distinct and have greater genomic potential to decay SOM.

Gene based calculation of community aggregated traits (CAT's) may be used to assess community-level microbial properties (Fierer *et al.*, 2014), CAT's are conceptually similar to widely used measures of community weighted mean (CWM) trait values for plant communities (Cornwell & Ackerly, 2009; Bernard-Verdier *et al.*, 2012). Because ectomycorrhizal fungi use decay mechanisms retained from their saprotrophic ancestors (Lindahl & Tunlid, 2015; Pellitier & Zak, 2018), genes found in saprotrophic fungal genomes encoding hydrolytic and oxidative enzymes, as well as Fenton-based decay mechanisms are likely involved in ECM fungal degradation of SOM (Doré *et al.*, 2015; Kohler *et al.*, 2015; Nicolás *et al.*, 2019; Floudas *et al.*, 2020). In most cases however, the identity and activity of specific gene families, particularly under field conditions, remain unknown (Zak *et al.*, 2019b). If gene families associated with SOM decay impact fungal persistence within a community (*i.e.* are functional) (Violle *et al.*, 2007), shifts in the relative abundance of certain gene families along the soil inorganic N

gradient could represent the outcome of assembly processes that favored or disfavored their suitability.

We studied ECM fungal communities inhabiting sixty even-aged *Quercus rubra* L. trees arrayed along a natural inorganic N gradient in a temperate upland forest ecosystem. We used amplicon sequencing to characterize shifts in ECM fungal communities and calculated community aggregated decay trait (CADT) profiles using shotgun metagenomic sequencing. We identified linkages between 100 individual gene families and soil inorganic N availability using an extension of indicator species (gene) analysis (Baker & King, 2010). Our use of a single and even-aged host (~100 years old) eliminates the potentially confounding effect of host specificity and ontogeny in fungal community assembly (Wasyliw and Karst 2020, van der Linde et al. 2018).

For fungal gene families that are primarily involved in SOM decay, we hypothesize negative correlations with increasing soil inorganic N availability. Specifically, extracellular class II peroxidases appear critical to ECM fungal decay under laboratory and field conditions (Bödeker *et al.*, 2014; Sterkenburg *et al.*, 2018; Lindahl *et al.*, 2021). Manganese peroxidases (MnP), lignin peroxidase (LiP) and dye-decoloring peroxidases (DxP), evolved exclusively in the Agaricomycetes and have some of the greatest known oxidative capacity to decay SOM (Janusz *et al.*, 2017). These genes are present at relatively high abundance in certain ECM fungal genomes, such as the widespread genus *Cortinarius* (Bödeker *et al.*, 2009; Miyauchi *et al.*, 2020). Additionally, genes encoding extracellular lytic polysaccharide monooxygenases (LPMOs) are upregulated in ECM fungal hyphae in the presence of SOM (Nicolás *et al.*, 2019). Finally, cellobiose dehydrogenases (CDH) are almost exclusively produced by white-rot saprotrophic fungi, and for ECM fungi that originated from such lineages CDH may play a substantial role in the decay of SOM (Doré *et al.*, 2015; Janusz *et al.*, 2017). In contrast, genes with primarily intracellular roles, such as initiation of the mycorrhizal symbiosis or fungal cell wall remodeling may not exhibit significant responses to the soil inorganic N gradient.

Materials and Methods:

Site Descriptions:

Sixty mature *Quercus rubra* L. individuals, were sampled across a natural mosaic of soil inorganic N availabilities in Manistee National Forest in northwestern Lower Michigan (Fig. S1).

Trees studied here are approximately even aged resulting from regrowth following forest clearing in the early 20th century; forests in this region have subsequently been free of anthropogenic disturbance. Five mature *Q. rubra* individuals that were at least 10 m apart were sampled within a total of 12 forest stands; previous studies indicate that these stands broadly span the range of soil nutrient availabilities in this region (Zak *et al.*, 1986; Zak & Pregitzer, 1990). Variation in nutrient cycling is derived from micro-site climatic differences in nutrient and water retention that have developed in the past ~10,000 yrs, and all focal trees occur within an elevation band of 70-130m (Zak *et al.*, 1986). Relative differences in soil nutrient availability among soils have persisted for decades (Zak *et al.*, 1986; Zak & Pregitzer, 1990). Soils across the study region are uniformly derived from sandy (~85% sand) glacial drift and because the sampling region is relatively small, with the most distant sites being ~50 km apart (Fig. S1), macroclimatic differences are minimal. Annual rates of net N mineralization, an estimate of inorganic N availability, range from 38 to 120 kg N ha^{-1} y^{-1} (calculated from Zak and Pregitzer 1990), which broadly spans soil inorganic N availability in the upper Lake States region (Pastor *et al.*, 1984; McClaugherty *et al.*, 1985). Nitrogen deposition in the study region based on National Atmospheric Deposition Program estimates (year 2016) is ~ 3kg N ha^{-1} primarily in the form of NH_4^+. Foliar N concentrations of the focal trees increased with soil mineralization rates ranging from 21-29 mg g^{-1} (Pellitier *et al.*, 2021). The regional scale (~50 km) of this study may reduce the potential for dispersal limitation to be an overwhelming impact on community assembly (Peay *et al.*, 2012), such that observed patterns in species and trait distributions primarily represent the outcome of differential biotic and abiotic filters on community assembly (Ackerly, 2003). See *Supplementary Methods* for further information.

Soil Characterization:

In August 2018, ECM fungal root-tips were collected radially around the dripline of each focal *Q. rubra* individual; cores were 10-cm deep and 144 cm^2 (11 x 11cm) and each of the five cores collected for each tree were kept intact until dissection. Soil cores for physico-chemical analysis were collected immediately adjacent to the root-tip cores in both May and August 2018, but were 5-cm diameter and 10-cm deep. O_i horizon was removed where present, ranging from 0.24-2cm across stands. Soil net N mineralization rates, soil C and N, pH, total free primary amines (TFPA), as well as gravimetric soil water content, were measured from these soil cores. In addition, all overstory plant stems greater than 5 cm diameter breast height (DBH), within 10 m

of each focal *Q. rubra* stem, were identified and measured at DBH. A total of 1,304 non-focal tree stems were inventoried. See *Supplementary Methods* for further detail.

Isolating Ectomycorrhizal fungal Root-tips:

Briefly, root-tip cores were pooled for each individual focal tree and root-tips were manually excised using a dissecting microscope after visually eliminating non-*Quercus* roots. Sampling was standardized by visually assessing the tips of ~ 90% (wet weight) of all *Quercus* roots in each of the root cores. In total, 14, 944 ECM fungal root-tips were excised. DNA was extracted from lyophilized tissue using the Qiagen DNeasy Plant Mini Kit (Hilden, Germany) and DNA pools were split for subsequent amplicon and metagenomic sequencing. See *Supplementary Methods* for further detail.

PCR and Fungal Taxonomy:

The ITS2 fragment of rRNA was amplified using PCR, following Taylor *et al.* (2016) and sequenced using Illumina Mi-Seq (2 x 250; San Diego, CA). Sequences were processed using DADA2 and amplicon sequence variants (ASV) were assigned taxonomy using the using the UNITE dynamic database (v.8; 97-99% sequence similarity) (Callahan *et al.*, 2016; Nilsson *et al.*, 2019). The mycorrhizal status of fungal genera was assigned using literature searches (Tedersoo & Smith, 2013), and genera with mixed, unidentified, or non-ECM fungal status were removed from subsequent analyses (~5% of overall sequences). We used the DEEMY (characterization and DEtermination of EctoMYcorrhizae) database (http://www.deemy.de/) to gather morphological information on the exploration type (hyphal foraging distance) and rhizomorph occurrence of taxa present in our dataset at more than 0.5% relative abundance. Taxa exclusively forming 'abundant' rhizomorphs, were scored as 'rhizomorphic', and all medium-distance exploration types, were defined as 'medium distance'. Overall, we assigned morphological hyphal data for 28 ECM fungal genera, comprising more than 93% of all identified ECM fungal sequences.

Metagenomic Sequence Generation, Processing and Annotation:

Shotgun metagenomic sequencing was conducted using a NovaSeq 6000 instrument (2 x 150bp) at the University of Michigan Advanced Genomics Core. In total, 23,203,326,006 metagenomic sequences were generated, and were not merged. Filtered sequences Q > 20 were mapped to the UniVec database (bacterial, archaeal, human, viral) sequences, as well as *Quercus rubra* (Konar *et al.*, 2017) and *Qurcus lobata* genome assemblies (Sork *et al.*, 2016) using Kraken2 with

default settings (v.2.0.8) (Wood *et al.*, 2019). On average, 21.7% of sequences per sample were removed during this filtering step, yielding a mean of 307,041,274 putative fungal sequences per sample. Next, we used a direct mapping approach to annotate sequences against the CAZy and Peroxibase reference databases (100 total gene families; Table S1) using 'sensitive' setting in DIAMOND with an -e value: $1e^{-4}$ (v.0.9.29) (Buchfink *et al.*, 2015) and BWA-MEM with standard settings (v.0.7.17) (Li & Durbin, 2009), following recommendations for unmerged reads (Treiber *et al.*, 2020). The compiled gene database primarily contained previously defined 'core' gene families found to be actively expressed during fungal decay of SOM (Peng *et al.*, 2018; Floudas *et al.*, 2020) (CAZy: http://www.cazy.org; http://peroxibase.toulouse.inra.fr/) (Table S1). We tabulated the number of near-single copy genes, as a proxy for the number of Dikaryotic genomes present in each sample, using the OrthoDB v.9 gene database, which comprised 1,312 near-single copy Dikaryotic gene variants (Kriventseva *et al.*, 2019). Further methodological details are presented in the *Supplementary Methods*.

Statistical Analysis:

ECM fungal communities were rarefied to an even depth (24,021 sequences) and the responses of individual fungal genera to net N mineralization rates was conducted using Threshold Indicator Taxa ANalysis using the 'TITAN2' package in R (Baker & King, 2010). We visualized variation in ECM fungal community composition using NMDS with the R package *vegan* v. 2.5.6 (Oksanen et al., 2020). To isolate the effect of net N mineralization and other soil parameters in driving shifts in community composition, we used generalized dissimilarity modeling (GDM) (Ferrier *et al.*, 2007; Duhamel *et al.*, 2019). Predictors initially included in the model were net N mineralization rates, pH, soil C and N, C:N, TFPA, gravimetric water availability and Bray-Curtis transformed plant overstory dissimilarity matrix (ran separately for stem frequency or stem frequencies weighted by diameter at breast height (DBH); this model incorporated geographic distances between individual focal trees to account for potential spatial autocorrelation. We used backwards model selection (Qin *et al.*, 2020), and confirmed the significance of remaining predictors using matrix permutation (*nperm* = 500).

Gene counts derived from community-level shotgun metagenomic sequencing are weighted by the relative abundance of taxa present (Fierer *et al.*, 2012, 2014; Quinn *et al.*, 2019). To account for the compositional nature of the metagenomic data, we calculated the natural logarithm of the number of sequences mapped to a given decay gene family divided by the

geometric mean number of near single-copy genes present in the sample (single-copy genes). Note that this is identical to an additive log-ratio transformation (Quinn *et al.*, 2018), which reveals how the relative abundance of decay genes present in a community behave relative to the number of single-copy genes (genomes) present in each sample. This allowed us to estimate, on average the potential decay capacity of a hypothetical, fungal genome in each community, thereby estimating a CADT (Fierer *et al.*, 2014). Note that shotgun metagenomics allows for assessment of genotypic trait variation independent of environment impacts on expression.

We employed an extension of GDM's to identify environmental and biotic predictors correlated with shifts in the compositional abundance of the 100 decay gene families. While this is the first known employment of GDM for metagenomic sequences, it is conceptually similar to modeling genomic variation across environmental gradients using single nucleotide polymorphisms (Fitzpatrick & Keller, 2015), or nucleotide percentages for assembled genomes (Bouma-Gregson *et al.*, 2019). Standardized gene counts were Hellinger transformed (without prior log-transformation) and Euclidean distances calculated; initial environmental predictors included those described above, as well as a Bray-Curtis dissimilarity matrix of ECM fungal community composition. We employed a similar modeling selection procedure as described above. A separate GDM was run and additionally included a dissimilarity matrix (Bray-Curtis) of non-mycorrhizal fungi present, including unidentified fungal sequences totaling 512 ASV.

We employed TITAN2 (Baker & King, 2010) to identify 'indicator' fungal gene families that responded to measures of net N mineralization using IndVal thresholds similar to previous studies of microbial 'omic responses to environmental gradients (Malik *et al.*, 2020b). We separately conducted models where soil C, and gravimetric water content were predictor variables. To account for potential non-independence among trees (samples) as a result of spatial proximity within stands, we accounted for the exact distance among trees using distances calculated from GPS coordinates. We used linear mixed effect (LME) models, taking into account the underlying spatial sampling structure, using a gaussian correlation structure as random effects. Euclidean distances among trees were calculated and restricted maximum likelihood estimation was conducted using the package nlme 3.1 (Pinheiro et al., 2017). Residuals were plotted to check for violations of normality. All statistical analyses were conducted in R v. 4.0.2.

Results:

The underlying soil inorganic N gradient measured using estimates of net N mineralization was temporally stable across the duration of the 2018 growing season (Fig. S2). The number of ECM fungal root-tips encountered, as well as their overall biomass, was inversely related with soil inorganic N availability (Fig. S3-4). We recovered a total of 202 ECM fungal ASV, comprising 44 genera, of which 88% were Basidiomycetes. The proportion of sequences attributed to ECM fungal taxa was greatest under conditions of low inorganic N availability ($P = 0.053$); however, this trend is likely driven by certain outliers because sequences that could not be identified at the genus level or had mixed trophic status such as (*Entoloma*) were not included (Tedersoo & Smith, 2013). Inclusion of *Entoloma*, resulted in weaker shift in the proportion of ECM fungal sequences recovered in each sample across the gradient ($P = 0.11$). Alpha diversity measured as observed ECM fungal ASV ranged from 9-50 taxa per sample, and declined significantly across the soil gradient, however Simpsons index was invariant (Fig. S5).

The morphological and compositional attributes of ECM fungal communities varied significantly across the soil inorganic N gradient (Figure 1). For example, the relative abundance of ectomycorrhizal fungi possessing medium distance exploration types ($R^2 = 0.16$, $P = 0.001$ linear fit; T= -3.50, $P = 0.0009$ spatial LME), and rhizomorphic hyphae were more prevalent in soils with low rates of net N mineralization ($R^2 = 0.13$, $P = 0.003$ linear fit; T= -2.94 , P=0.0047 spatial LME; Figure 1). Importantly, the proportion of ECM fungal sequences assigned morphological attributes using DEEMY did not vary across samples ($P = 0.50$). GDM revealed that shifts in ECM fungal community composition were well explained by soil pH, rates of net N mineralization and C:N, together explaining 36% of model deviance (Figure 2; Table S2).

The number of metagenomic sequences that passed quality filtering steps and the sequences remaining after removal of plant and non-fungal contaminants did not significantly vary across the soil inorganic N gradient ($P = 0.36$; Fig. S6; Table S3), nor did the geometric mean number of single-copy gene sequences ($P = 0.17$; Fig. S7). The standard error of single-copy sequences in each sample, a coarse metric of the evenness of genome coverage per community, also did not significantly vary ($P = 0.76$). To qualitatively compare amplicon and metagenomic based estimates of fungal alpha diversity, we regressed the mean number of fungal genomes estimated using OrthoDB from metagenomic libraries against both the number of observed ECM fungal ASV, as well as the total number of fungal ASV; we observed no trends

for either relationship (Fig. S8). While we cannot conclusively determine that all sequences attributed to various CAZy gene families have an ECM fungal origin, only a small proportion of non-ECM fungi (~5%) were encountered in our amplicon libraries (SE=0.007).

We observed shifts in the relative abundance of fungal gene families active on different substrates present in SOM across the soil inorganic N gradient (Figure 3). The presence of genes encoding enzymes active on lignin, cellulose and chitin were greatest under conditions of low inorganic N availability (Figure 3). For example, genes active on cellulose and chitin were 5.2 and 3.0 times more abundant under conditions of low inorganic N availability. More specifically, the relative abundance of fungal class II peroxidases and lytic polysaccharide moonoxygenases (LPMO) decreased with increasing rates of net N mineralization rates (Figure 4). Mn-peroxidases were 4.9 times more abundant and genes encoding LPMO were 2.7 times more abundant under conditions of low inorganic N availability. A total of 35 fungal gene families (Fig. S9) were identified as responsive to net N mineralization rates, including positive (n = 20) and negative (n = 15) indictor gene families (Figure 5); many of these fungal gene families were also identified as responsive to soil C and gravimetric water content (Fig. S9-11). The summed abundance of 'indicator' fungal genes that responded negatively to increasing rates of net N mineralization was significantly greater than those that responded positively to inorganic N availability (T-test: T = -12.68, $P < 0.0001$; Figure 5).

GDM analyses revealed that soil C, gravimetric water content, and ECM fungal community dissimilarity were significant predictors of shifts in the compositional abundance of metagenomic gene families (Figure 2). Together, these predictors accounted for ~ 22% of model variance; ECM fungal community dissimilarity explained ~ 63% of observed model deviance (P = 0.066; Data S2). However, when ECM fungal community composition was removed as a predictor, rates of net N mineralization were not a significant predictor of dissimilarity in fungal metagenomic composition. Finally, because non-ECM fungal taxa could potentially account for shifts in community gene counts (Fig. S12), we incorporated both ECM fungal and non-ECM fungal community dissimilarity matrices into a separate GDM; this model explained 27% of model deviance (Table S2; Fig. S13). Relationships between the relative abundance of individual fungal gene families and rates of net N mineralization, soil C, and gravimetric water content are reported in Table S4. The relative sequence abundance of fungal taxa forming rhizomorphic hyphae (T= 1.39, P= 0.17) and medium distance exploration types (T = 1.66, P = 0.10) was

positively correlated with the abundance of fungal gene families that exhibited negative responses to rates of net N mineralization (negative indicator fungal gene families; n=15) (Figure 6). Negative indicator fungal gene families were 4.2 and 4.9 times more abundant where fungal taxa forming rhizomorphic hyphae and medium distance exploration types were most common. Finally, the relative abundance of ECM fungi in the genus *Cortinarius* was positively associated with the summed abundance of negative 'indicator' fungal gene families (Figure 7).

Discussion:

ECM fungal assimilation of various N forms has been deemed both a response and effect trait, which simultaneously impacts the outcome of assembly processes and consequentially, ecosystem function (Koide *et al.*, 2014). In this study, we document coupled shifts in ECM fungal community composition and community level fungal gene frequencies associated with SOM decay along a soil inorganic N gradient. These findings provide support for the primacy of N acquisition strategies, particularly SOM decay, in mediating ECM fungal community assembly. Overall, ECM fungal communities occurring in low inorganic N soils possessed greater genomic potential to decay SOM and the abundance of gene families that operate on components of SOM (lignin, chitin and cellulose) were most abundant under these conditions. While these patterns are not causative relationships, they are congruent with models of dynamic plant adaptation to nitrogen limited condition via symbiosis with specialized ECM fungal communities that may obtain N-SOM. When considered alongside paired studies of *Q. rubra* response to increasing CO_2 (Pellitier et al., *in press*), our results suggest the context-dependent contribution of N-SOM to plant growth which expands existing mycorrhizal nutrient economic paradigms (Phillips *et al.*, 2013).

ECM fungal community composition was the primary determinant of fungal decay gene frequencies. Moreover, inorganic N availability was a significant driver of ECM fungal community composition and may therefore act as a primary determinant of these taxonomic and functional gene shifts. Such a finding is notable because ECM fungal community turnover along both natural and polluted soil N availability gradients has been repeatedly demonstrated (Lilleskov *et al.*, 2002a; Toljander *et al.*, 2006; Cox *et al.*, 2010; van der Linde *et al.*, 2018) whereas functional shifts along soil N gradients remains poorly studied (Lilleskov *et al.*, 2002b). Overall, ECM fungal communities with the greatest decay potential were dominated by the

genera *Cortinarius* and *Hebeloma*. These genera have retained some of the highest quantity of fungal genes involved in SOM decay (Bödeker *et al.*, 2009; Kohler *et al.*, 2015). We found significant correlations between the relative abundance of *Cortinarius* amplicons and the abundance of fungal genes encoding manganese peroxidases (MnP), building towards a functional perspective on the ecological niche of this widespread and diverse genus. *Cortinarius* is consistently found in low inorganic N soils (Sterkenburg *et al.*, 2015; van der Linde *et al.*, 2018) and our results are congruent with findings that this genus may actively decay SOM (Lindahl *et al.*, 2021). In contrast, so-called nitrophilic genera, commonly observed under conditions of high inorganic N availability, such as certain *Scleroderma* and *Russula* (Avis, 2012; van der Linde *et al.*, 2018), are here associated with lesser capacity to degrade SOM (Bödeker *et al.*, 2009; Kohler *et al.*, 2015; Miyauchi *et al.*, 2020). Although not part of this study, ECM fungal taxa associated with high inorganic N soils may be enriched in high affinity membrane transporters that efficiently acquire NH_4 and NO_3 (Javelle *et al.*, 2003; Kranabetter *et al.*, 2015).

Hyphal morpho-traits associated with N foraging exhibited parallel shifts with ECM fungal community composition and metagenomic decay potential. Taxa forming rhizomorphic and medium-distance exploration strategies dominated under conditions of low inorganic N availability. By linking metagenomic measurements of ECM fungal decay potential with turnover in hyphal morpho-traits, our study broadly supports the hypothesized, role of these hyphal morphologies in the decay of SOM (Hobbie & Agerer, 2010; Moeller *et al.*, 2014; Defrenne *et al.*, 2019). Our findings are also consistent with suggestions that fungal taxa forming rhizomorphic hyphae are strong competitors in conditions where plant access to inorganic N is scarce (Defrenne *et al.*, 2019). Such observations contribute to predictions that plants dynamically allocate to C to ECM fungal symbionts that efficiently forage for N, whilst minimizing C cost (Koide *et al.*, 2014; van der Linde *et al.*, 2018).

Certain gene families with high oxidative potential occurred at greater abundance in conditions of low inorganic N availability, particularly those encoding lytic polysaccharide monooxygenases (LPMOs – AA9,10,11,13) and manganese and dye decoloring peroxidases (MnP; DyPrx). These findings provide certain support for the hypothesis that ECM fungal decay potential, and potentially the acquisition of N-SOM, is greatest under conditions of low inorganic N availability. LPMOs and MnP encode primarily extracellular enzymes enabling the decay of

SOM (Villares *et al.*, 2017; Janusz *et al.*, 2017) and have been the subject of recent investigations of ECM fungal SOM decay under laboratory (Doré *et al.*, 2015; Kohler *et al.*, 2015; Shah *et al.*, 2016; Nicolás *et al.*, 2019) and field conditions (Bödeker *et al.*, 2014; Sterkenburg *et al.*, 2018; Lindahl *et al.*, 2021). In addition, cellobiose dehydrogenase catalyzes the production of H_2O_2 (Janusz *et al.*, 2017; Sützl *et al.*, 2018) necessary for MnP (Hammel & Cullen, 2008) and LPMO activity (Sützl *et al.*, 2018); these gene families (AA3_1 and AA3_2) also declined significantly with increasing soil inorganic N availability. Overall, our results highlight MnP, one of the most potent fungal decay enzyme classes (Janusz *et al.*, 2017), as likely playing a key role in ECM fungal decay of SOM (Bödeker *et al.*, 2014; Zak *et al.*, 2019a; Lindahl *et al.*, 2021) and builds toward predictive understanding of the environmental controls governing the distribution of this decay pathway (Bödeker *et al.*, 2014; Sterkenburg *et al.*, 2018). Additionally, gene families such as CE4, CE9, and GH23 which are active on peptidoglycan also responded negatively to increasing soil inorganic N availability. Overall, the concomitant shifts in a wide array of decay gene families along the gradient of soil inorganic N availability is notable because it supports the existence of multiple, yet potentially coupled enzymatic decay pathways that ECM fungal communities may employ to decay the diversity of plant and microbial compounds composing SOM. Unfortunately, gene families involved in non-enzymatic Fenton decay mechanisms remain ambiguous and further study is critical to resolve this decay process (Shah *et al.*, 2016; Janusz *et al.*, 2017; Sützl *et al.*, 2018).

Certain CAZy gene families, which are not 'functional' with respect to fitness outcomes (Shipley *et al.*, 2016), may not exhibit significant shifts across environmental gradients (Ackerly, 2003). In fact, the majority of gene families studied here exhibited minimal shifts across the inorganic N availability gradient. This does not necessarily suggest that ECM fungal communities are broadly equivalent in their capacity to decay SOM. Metagenomic investigations of microbial functional traits are generally limited by their inability to link gene frequencies with phenotypes, limiting complete understanding of trait-based environmental filtering processes shaping these communities (Ackerly, 2003). Further investigation of transcriptional regulation, and enzymatic expression linked with plant uptake of N-SOM are required to fully understand plant acquisition of this critical limiting nutrient. Finally, it is critical to point out that annotation of ECM fungal genes involved in the decay of SOM is a substantial challenge because ECM

fungi remain poorly represented relative to saprotrophic and pathogenic fungi in available databases.

Alongside gene families that exhibited negative and neutral responses, we observed numerous gene families that were positively correlated with increasing soil inorganic N availability. Evaluating these findings with the prevailing compositional and morphological patterns is challenging. However, certain gene families that exhibited this pattern have ambiguous activity that may not be directly involved in SOM decay. For example, certain GH5 and CE8 may play a role in mycorrhizal initiation, morphogenesis, remodeling of the fungal cell wall or cell wall polysaccharide branching (Kües & Rühl, 2011; Blatzer *et al.*, 2020; Genre *et al.*, 2020). Gene families targeting hemi-cellulose also increased in relative abundance, as well as those releasing N from chitin (GH18 and GH20). We also acknowledge that certain gene families which exhibited negative responses to soil inorganic N availability, could also have alternative functions such as chitin remodeling in the fungal cell wall (AA9 or AA11).

Capturing the role of microbial communities on host tree nutrition or other biogeochemical processes (Averill *et al.*, 2014; Sulman *et al.*, 2019) requires scaling gene frequencies by estimates of microbial abundance. Similar to other studies, we documented that the number of ECM fungal root-tips decreased substantially with increasing inorganic N availability (Nilsson *et al.*, 2005; Högberg *et al.*, 2017). Qualitative scaling of genomic estimates of CADT by root-tip abundance further emphasizes the greater potential of ECM fungi occurring in inorganic N poor soils to decay SOM. While we stress that we did not directly measure plant uptake of N-SOM, the metagenomic patterns we revealed are consistent with previous isotopic study of the same *Q. rubra* individuals. In a complementary study, we found highly ^{15}N depleted foliage for *Q. rubra* growing under conditions of low inorganic N availability, and enriched foliage for *Q. rubra* occupying soils with high inorganic N availability (Pellitier *et al.*, 2021); these patterns are consistent with a transition from plant reliance on N-SOM to inorganic N uptake (Kranabetter & MacKenzie, 2010).

This work represents one of the first to identify gene-trait environment linkages for microorganisms under field settings (Satinsky *et al.*, 2017; Rath *et al.*, 2019; Bouma-Gregson *et al.*, 2019; Malik *et al.*, 2020b). Consistent with expectations of trait-mediated assembly processes, metagenomic measurements of ECM fungal decay potential were associated with shifts in overall ECM fungal community composition. Our work provides unique support for the

hypothesis that ECM fungi with enhanced SOM decay capacity are favored under conditions of low inorganic N availability (Koide *et al.*, 2014). Our observations of shifts in the functional attributes of ECM fungal communities could represent a mechanistic basis for flexibility in plant nutrient foraging along soil N gradients, and thereby expands understanding of the organic N cycle (Kielland, 1994; Nordin *et al.*, 2004; Näsholm *et al.*, 2009). In a seminal viewpoint, Read and Perez Moreno (2003) suggested that the capacity of ECM fungi to obtain N-SOM may control the biogeography of the ECM fungal symbiosis. Our results highlight that the decay attributes of ECM fungal taxa may structure their distribution along soil inorganic N gradients.

Acknowledgements: We thank R. Upchurch, E. Herrick, K. Seguin, N. Gudal, N. Ahmad, B. VanDusen and W. Argiroff for valuable laboratory and field support. V. Denef, M. Coon, J. Evans and T. James provided essential sequencing and bioinformatic support. D. Goldberg and K. Peay provided comments on a draft of this manuscript. This work is supported by NSF award 1754369, and an Integrated Training in Microbial Systems (ITiMS) Fellowship to PTP. The authors declare no competing interests.

Author Contributions: PTP and DRZ designed the study. PTP collected and analyzed data, and wrote the manuscript with contributions from DRZ.

Data Availability: Raw DNA sequences associated with the ITS2 amplicon sequencing are deposited in NCBI Sequence Read Archive: SRR14164239-SRR14164298. Metagenomic sequences are deposited under accession codes: SRR15377920-SRR15377978. Associated soil metadata are available in Dryad (https://doi.org/ 10.5061/dryad.4f4qrfjbt).

References:

Ackerly DD. **2003**. Community Assembly, Niche Conservatism, and Adaptive Evolution in Changing Environments. *International Journal of Plant Sciences* **164**: S165–S184.

Ackerly DD, Cornwell WK. **2007**. A trait-based approach to community assembly: partitioning of species trait values into within- and among-community components. *Ecology Letters* **10**: 135–145.

Averill C, Turner BL, Finzi AC. **2014**. Mycorrhiza-mediated competition between plants and decomposers drives soil carbon storage. *Nature* **505**: 543–545.

Avis PG. **2012**. Ectomycorrhizal iconoclasts: the ITS rDNA diversity and nitrophilic tendencies of fetid Russula. *Mycologia* **104**: 998–1007.

Baker ME, King RS. **2010**. A new method for detecting and interpreting biodiversity and ecological community thresholds. *Methods in Ecology and Evolution* **1**: 25–37.

Bernard-Verdier M, Navas M-L, Vellend M, Violle C, Fayolle A, Garnier E. **2012**. Community assembly along a soil depth gradient: contrasting patterns of plant trait convergence and divergence in a Mediterranean rangeland. *Journal of Ecology* **100**: 1422–1433.

Blatzer M, Beauvais A, Henrissat B, Latgé J-P. **2020**. Revisiting Old Questions and New Approaches to Investigate the Fungal Cell Wall Construction. In: Latgé JP. (eds) Current Topics in Microbiology and Immunology vol 425. Berlin, Heidelberg: Springer Berlin Heidelberg, 331-369.

Bödeker ITM, Clemmensen KE, Boer W de, Martin F, Olson Å, Lindahl BD. **2014**. Ectomycorrhizal *Cortinarius* species participate in enzymatic oxidation of humus in northern forest ecosystems. *New Phytologist* **203**: 245–256.

Bödeker ITM, Nygren CMR, Taylor AFS, Olson Å, Lindahl BD. **2009**. ClassII peroxidase-encoding genes are present in a phylogenetically wide range of ectomycorrhizal fungi. *The ISME Journal* **3**: 1387–1395.

Bogar L, Peay K, Kornfeld A, Huggins J, Hortal S, Anderson I, Kennedy P. **2019**. Plant-mediated partner discrimination in ectomycorrhizal mutualisms. *Mycorrhiza* **29**: 97–111.

Bouma-Gregson K, Olm MR, Probst AJ, Anantharaman K, Power ME, Banfield JF. **2019**. Impacts of microbial assemblage and environmental conditions on the distribution of anatoxin-a producing cyanobacteria within a river network. *The ISME Journal* **13**: 1618–1634.

Bradford MA, Wood SA, Addicott ET, Fenichel EP, Fields N, González-Rivero J, Jevon FV, Maynard DS, Oldfield EE, Polussa A, *et al.* 2021. Quantifying microbial control of soil organic matter dynamics at macrosystem scales. *Biogeochemistry*. doi: 10.1007/s10533-021-00789-5.

Buchfink B, Xie C, Huson DH. **2015**. Fast and sensitive protein alignment using DIAMOND. *Nature Methods* **12**: 59–60.

Callahan BJ, McMurdie PJ, Rosen MJ, Han AW, Johnson AJA, Holmes SP. **2016**. DADA2: High-resolution sample inference from Illumina amplicon data. *Nature Methods* **13**: 581–583.

Christian N, Bever JD. **2018**. Carbon allocation and competition maintain variation in plant root mutualisms. *Ecology and Evolution* **8**: 5792–5800.

Cornwell WK, Ackerly DD. **2009**. Community assembly and shifts in plant trait distributions across an environmental gradient in coastal California. *Ecological Monographs* **79**: 109–126.

Courty P-E, François M, Marc-André S, Myriam D, Criquet Stéven, Fabio Z, Marc B, Claude P, Adrien T, Jean G, *et al.* 2016. Into the functional ecology of ectomycorrhizal communities: environmental filtering of enzymatic activities. *Journal of Ecology* **104**: 1585–1598.

Cox F, Barsoum N, Lilleskov EA, Bidartondo MI. **2010**. Nitrogen availability is a primary determinant of conifer mycorrhizas across complex environmental gradients. *Ecology Letters* **13**: 1103–1113.

Defrenne CE, Philpott TJ, Guichon SHA, Roach WJ, Pickles BJ, Simard SW. **2019**. Shifts in Ectomycorrhizal Fungal Communities and Exploration Types Relate to the Environment and Fine-Root Traits Across Interior Douglas-Fir Forests of Western Canada. *Frontiers in Plant Science* **10**: 643.

Diaz S, Cabido M, Casanoves F. **1998**. Plant functional traits and environmental filters at a regional scale. *Journal of Vegetation Science* **9**: 113–122.

Doré J, Perraud M, Dieryckx C, Kohler A, Morin E, Henrissat B, Lindquist E, Zimmermann SD, Girard V, Kuo A, *et al.* 2015. Comparative genomics, proteomics and transcriptomics give new insight into the exoproteome of the basidiomycete *Hebeloma cylindrosporum* and its involvement in ectomycorrhizal symbiosis. *New Phytologist* **208**: 1169–1187.

Duhamel M, Wan J, Bogar LM, Segnitz RM, Duncritts NC, Peay KG. **2019**. Plant selection initiates alternative successional trajectories in the soil microbial community after disturbance. *Ecological Monographs* **89**: e01367.

Ferrier S, Manion G, Elith J, Richardson K. **2007**. Using generalized dissimilarity modelling to analyse and predict patterns of beta diversity in regional biodiversity assessment. *Diversity and Distributions* **13**: 252–264.

Fierer N, Barberán A, Laughlin DC. **2014**. Seeing the forest for the genes: using metagenomics to infer the aggregated traits of microbial communities. *Frontiers in Microbiology* **5**.614

Fierer N, Leff JW, Adams BJ, Nielsen UN, Bates ST, Lauber CL, Owens S, Gilbert JA, Wall DH, Caporaso JG. **2012**. Cross-biome metagenomic analyses of soil microbial communities and their functional attributes. *Proceedings of the National Academy of Sciences* **109**: 21390–21395.

Fitzpatrick CR, Copeland J, Wang PW, Guttman DS, Kotanen PM, Johnson MTJ. **2018**. Assembly and ecological function of the root microbiome across angiosperm plant species. *Proceedings of the National Academy of Sciences* **115**: E1157–E1165.

Fitzpatrick MC, Keller SR. **2015**. Ecological genomics meets community-level modelling of biodiversity: mapping the genomic landscape of current and future environmental adaptation. *Ecology Letters* **18**: 1–16.

Floudas D, Bentzer J, Ahrén D, Johansson T, Persson P, Tunlid A. **2020**. Uncovering the hidden diversity of litter-decomposition mechanisms in mushroom-forming fungi. *The ISME Journal*. **14:** 2046-2059

Fry EL, Long JRD, Garrido LÁ, Alvarez N, Carrillo Y, Castañeda-Gómez L, Chomel M, Dondini M, Drake JE, Hasegawa S, *et al.* 2019. Using plant, microbe, and soil fauna traits to improve the predictive power of biogeochemical models. *Methods in Ecology and Evolution* **10**: 146–157.

Genre A, Lanfranco L, Perotto S, Bonfante P. **2020**. Unique and common traits in mycorrhizal symbioses. *Nature Reviews Microbiology*.**18:** 1659-1660

Hall EK, Bernhardt ES, Bier RL, Bradford MA, Boot CM, Cotner JB, del Giorgio PA, Evans SE, Graham EB, Jones SE, *et al.* 2018. Understanding how microbiomes influence the systems they inhabit. *Nature Microbiology* **3**: 977–982.

Hammel KE, Cullen D. **2008**. Role of fungal peroxidases in biological ligninolysis. *Current Opinion in Plant Biology* **11**: 349–355.

Hobbie EA, Agerer R. **2010**. Nitrogen isotopes in ectomycorrhizal sporocarps correspond to belowground exploration types. *Plant and Soil* **327**: 71–83.

Högberg P, Näsholm T, Franklin O, Högberg MN. **2017**. Tamm Review: On the nature of the nitrogen limitation to plant growth in Fennoscandian boreal forests. *Forest Ecology and Management* **403**: 161–185.

Hortal S, Plett KL, Plett JM, Cresswell T, Johansen M, Pendall E, Anderson IC. **2017**. Role of plant–fungal nutrient trading and host control in determining the competitive success of ectomycorrhizal fungi. *The ISME Journal* **11**: 2666–2676.

Janusz G, Pawlik A, Sulej J, Świderska-Burek U, Jarosz-Wilkołazka A, Paszczyński A. **2017**. Lignin degradation: microorganisms, enzymes involved, genomes analysis and evolution. *FEMS Microbiology Reviews* **41**: 941–962.

Javelle A, André B, Marini A-M, Chalot M. **2003**. High-affinity ammonium transporters and nitrogen sensing in mycorrhizas. *Trends in Microbiology* **11**: 53–55.

Kielland K. **1994**. Amino Acid Absorption by Arctic Plants: Implications for Plant Nutrition and Nitrogen Cycling. *Ecology* **75**: 2373–2383.

Kohler A, Kuo A, Nagy LG, Morin E, Barry KW, Buscot F, Canbäck B, Choi C, Cichocki N, Clum A, *et al.* 2015. Convergent losses of decay mechanisms and rapid turnover of symbiosis genes in mycorrhizal mutualists. *Nature Genetics* **47**: 410–415.

Koide RT, Fernandez C, Malcolm G. **2014**. Determining place and process: functional traits of ectomycorrhizal fungi that affect both community structure and ecosystem function. *New Phytologist* **201**: 433–439.

Konar A, Choudhury O, Bullis R, Fiedler L, Kruser JM, Stephens MT, Gailing O, Schlarbaum S, Coggeshall MV, Staton ME, *et al.* 2017. High-quality genetic mapping with ddRADseq in the non-model tree Quercus rubra. *BMC Genomics* **18**: 417.

Kranabetter JM, Hawkins BJ, Jones MD, Robbins S, Dyer T, Li T. **2015**. Species turnover (β-diversity) in ectomycorrhizal fungi linked to uptake capacity. *Molecular Ecology* **24**: 5992–6005.

Kranabetter JM, MacKenzie WH. **2010**. Contrasts Among Mycorrhizal Plant Guilds in Foliar Nitrogen Concentration and $\delta^{15}N$ Along Productivity Gradients of a Boreal Forest. *Ecosystems* **13**: 108–117.

Kriventseva EV, Kuznetsov D, Tegenfeldt F, Manni M, Dias R, Simão FA, Zdobnov EM. **2019**. OrthoDB v10: sampling the diversity of animal, plant, fungal, protist, bacterial and viral genomes for evolutionary and functional annotations of orthologs. *Nucleic Acids Research* **47**: D807–D811.

Kües U, Rühl M. **2011**. Multiple Multi-Copper Oxidase Gene Families in Basidiomycetes – What for? *Current Genomics* **12**: 72–94.

Lehmann J, Hansel CM, Kaiser C, Kleber M, Maher K, Manzoni S, Nunan N, Reichstein M, Schimel JP, Torn MS, *et al.* 2020. Persistence of soil organic carbon caused by functional complexity. *Nature Geoscience* **13**: 529–534.

Li H, Durbin R. **2009**. Fast and accurate short read alignment with Burrows–Wheeler transform. *Bioinformatics* **25**: 1754–1760.

Lilleskov EA, Fahey TJ, Horton TR, Lovett GM. **2002a**. Belowground Ectomycorrhizal Fungal Community Change Over a Nitrogen Deposition Gradient in Alaska. *Ecology* **83**: 104–115.

Lilleskov EA, Hobbie EA, Fahey TJ. **2002b**. Ectomycorrhizal fungal taxa differing in response to nitrogen deposition also differ in pure culture organic nitrogen use and natural abundance of nitrogen isotopes. *New Phytologist* **154**: 219–231.

Lindahl BD, Kyaschenko J, Varenius K, Clemmensen KE, Dahlberg A, Karltun E, Stendahl J. **2021**. A group of ectomycorrhizal fungi restricts organic matter accumulation in boreal forest. *Ecology Letters* **24**: 1341–1351.

Lindahl BD, Tunlid A. **2015**. Ectomycorrhizal fungi – potential organic matter decomposers, yet not saprotrophs. *The New Phytologist* **205**: 1443–1447.

van der Linde S, Suz LM, Orme CDL, Cox F, Andreae H, Asi E, Atkinson B, Benham S, Carroll C, Cools N, *et al.* 2018. Environment and host as large-scale controls of ectomycorrhizal fungi. *Nature* **558**: 243–248.

Malik AA, Martiny JBH, Brodie EL, Martiny AC, Treseder KK, Allison SD. **2020a**. Defining trait-based microbial strategies with consequences for soil carbon cycling under climate change. *The ISME Journal* **14**: 1–9.

Malik AA, Swenson T, Weihe C, Morrison EW, Martiny JBH, Brodie EL, Northen TR, Allison SD. **2020b**. Drought and plant litter chemistry alter microbial gene expression and metabolite production. *The ISME Journal*. **14**: 2236-2247

Maynard DS, Bradford MA, Covey KR, Lindner D, Glaeser J, Talbert DA, Tinker PJ, Walker DM, Crowther TW. **2019**. Consistent trade-offs in fungal trait expression across broad spatial scales. *Nature Microbiology* **4**: 846–853.

McClaugherty CA, Pastor J, Aber JD, Melillo JM. **1985**. Forest Litter Decomposition in Relation to Soil Nitrogen Dynamics and Litter Quality. *Ecology* **66**: 266–275.

Meeds JA, Marty Kranabetter J, Zigg I, Dunn D, Miros F, Shipley P, Jones MD. **2021**. Phosphorus deficiencies invoke optimal allocation of exoenzymes by ectomycorrhizas. *The ISME Journal*.**15:** 1478-1489

Miyauchi S, Kiss E, Kuo A, Drula E, Kohler A, Sánchez-García M, Morin E, Andreopoulos B, Barry KW, Bonito G, *et al.* 2020. Large-scale genome sequencing of mycorrhizal fungi provides insights into the early evolution of symbiotic traits. *Nature Communications* **11**: 5125.

Moeller HV, Peay KG, Fukami T. **2014**. Ectomycorrhizal fungal traits reflect environmental conditions along a coastal California edaphic gradient. *FEMS Microbiology Ecology* **87**: 797–806.

Näsholm T, Kielland K, Ganeteg U. **2009**. Uptake of organic nitrogen by plants. *New Phytologist* **182**: 31–48.

Nemergut DR, Schmidt SK, Fukami T, O'Neill SP, Bilinski TM, Stanish LF, Knelman JE, Darcy JL, Lynch RC, Wickey P, *et al.* 2013. Patterns and Processes of Microbial Community Assembly. *Microbiology and Molecular Biology Reviews* **77**: 342–356.

Nicolás C, Martin-Bertelsen T, Floudas D, Bentzer J, Smits M, Johansson T, Troein C, Persson P, Tunlid A. **2019**. The soil organic matter decomposition mechanisms in ectomycorrhizal fungi are tuned for liberating soil organic nitrogen. *The ISME Journal* **13**: 977–988.

Nilsson LO, Giesler R, Bååth E, Wallander H. **2005**. Growth and biomass of mycorrhizal mycelia in coniferous forests along short natural nutrient gradients. *New Phytologist* **165**: 613–622.

Nilsson RH, Larsson K-H, Taylor AFS, Bengtsson-Palme J, Jeppesen TS, Schigel D, Kennedy P, Picard K, Glöckner FO, Tedersoo L, *et al.* 2019. The UNITE database for molecular identification of fungi: handling dark taxa and parallel taxonomic classifications. *Nucleic Acids Research* **47**: D259–D264.

Nordin A, Schmidt IK, Shaver GR. **2004**. Nitrogen Uptake by Arctic Soil Microbes and Plants in Relation to Soil Nitrogen Supply. *Ecology* **85**: 955–962.

Orwin KH, Kirschbaum MUF, John MGS, Dickie IA. **2011**. Organic nutrient uptake by mycorrhizal fungi enhances ecosystem carbon storage: a model-based assessment. *Ecology Letters* **14**: 493–502.

Oksanen, J., Kindt, R., Legendre, P., O'Hara, B., Stevens, M.H.H., Oksanen, M.J. and Suggests, M.A.S.S., 2007. The vegan package. *Community ecology package*, **10:** 31-637

Pastor J, Aber JD, McClaugherty CA, Melillo JM. **1984**. Aboveground Production and N and P Cycling Along a Nitrogen Mineralization Gradient on Blackhawk Island, Wisconsin. *Ecology* **65**: 256–268.

Peay KG. **2016**. The Mutualistic Niche: Mycorrhizal Symbiosis and Community Dynamics. *Annual Review of Ecology, Evolution, and Systematics* **47**: 143–164.

Peay KG, Russo SE, McGuire KL, Lim Z, Chan JP, Tan S, Davies SJ. **2015**. Lack of host specificity leads to independent assortment of dipterocarps and ectomycorrhizal fungi across a soil fertility gradient. *Ecology Letters* **18**: 807–816.

Peay KG, Schubert MG, Nguyen NH, Bruns TD. **2012**. Measuring ectomycorrhizal fungal dispersal: macroecological patterns driven by microscopic propagules. *Molecular Ecology* **21**: 4122–4136.

Pellitier PT, Zak DR. **2018**. Ectomycorrhizal fungi and the enzymatic liberation of nitrogen from soil organic matter: why evolutionary history matters. *New Phytologist* **217**: 68–73.

Pellitier PT, Zak DR, Argiroff WA, Upchurch RA. **2021**. Coupled shifts in ectomycorrhizal communities and plant uptake of organic nitrogen along a soil gradient: an isotopic perspective. *Ecosystems*. doi: 10.1007/s10021-021-00628-6

Pellitier PT, Ibáñez I, Zak DR, Argiroff WA, Acharya, K. 2021. Ectomycorrhizal access to organic nitrogen mediates CO_2 fertilization response in a dominant tree species. *Nature Communications*. In press.

Peng M, Aguilar-Pontes MV, Hainaut M, Henrissat B, Hildén K, Mäkelä MR, de Vries RP. **2018**. Comparative analysis of basidiomycete transcriptomes reveals a core set of expressed genes encoding plant biomass degrading enzymes. *Fungal Genetics and Biology* **112**: 40–46.

Phillips RP, Brzostek E, Midgley MG. **2013**. The mycorrhizal-associated nutrient economy: a new framework for predicting carbon–nutrient couplings in temperate forests. *New Phytologist* **199**: 41–51.

Qin C, Zhu K, Chiariello NR, Field CB, Peay KG. **2020**. Fire history and plant community composition outweigh decadal multi-factor global change as drivers of microbial composition in an annual grassland. *Journal of Ecology* **108**: 611–625.

Quinn TP, Erb I, Gloor G, Notredame C, Richardson MF, Crowley TM. **2019**. A field guide for the compositional analysis of any-omics data. *GigaScience* **8**: giz107.

Quinn TP, Erb I, Richardson MF, Crowley TM. **2018**. Understanding sequencing data as compositions: an outlook and review (J Wren, Ed.). *Bioinformatics* **34**: 2870–2878.

Rath KM, Fierer N, Murphy DV, Rousk J. **2019**. Linking bacterial community composition to soil salinity along environmental gradients. *The ISME Journal* **13**: 836–846.

Ravanbakhsh M, Kowalchuk GA, Jousset A. **2019**. Root-associated microorganisms reprogram plant life history along the growth–stress resistance tradeoff. *The ISME Journal* **13**: 3093–3101.

Read DJ, Perez-Moreno J. **2003**. Mycorrhizas and Nutrient Cycling in Ecosystems: A Journey towards Relevance? *The New Phytologist* **157**: 475–492.

Satinsky BM, Smith CB, Sharma S, Landa M, Medeiros PM, Coles VJ, Yager PL, Crump BC, Moran MA. **2017**. Expression patterns of elemental cycling genes in the Amazon River Plume. *The ISME Journal* **11**: 1852–1864.

Schimel JP, Bennett J. **2004**. Nitrogen Mineralization: Challenges of a Changing Paradigm. *Ecology* **85**: 591–602.

Shah F, Nicolás C, Bentzer J, Ellström M, Smits M, Rineau F, Canbäck B, Floudas D, Carleer R, Lackner G, *et al.* 2016. Ectomycorrhizal fungi decompose soil organic matter using oxidative mechanisms adapted from saprotrophic ancestors. *New Phytologist* **209**: 1705–1719.

Shipley B, De Bello F, Cornelissen JHC, Laliberté E, Laughlin DC, Reich PB. **2016**. Reinforcing loose foundation stones in trait-based plant ecology. *Oecologia* **180**: 923–931.

Smith SE, Read DJ. **2010**. *Mycorrhizal symbiosis*. Academic press. USA

Sork VL, Fitz-Gibbon ST, Puiu D, Crepeau M, Gugger PF, Sherman R, Stevens K, Langley CH, Pellegrini M, Salzberg SL. **2016**. First Draft Assembly and Annotation of the Genome of a California Endemic Oak. *Genes|Genomes|Genetics* **6**: 3485–3495.

Sterkenburg E, Bahr A, Durling MB, Clemmensen KE, Lindahl BD. **2015**. Changes in fungal communities along a boreal forest soil fertility gradient. *New Phytologist* **207**: 1145–1158.

Sterkenburg E, Clemmensen KE, Ekblad A, Finlay RD, Lindahl BD. **2018**. Contrasting effects of ectomycorrhizal fungi on early and late stage decomposition in a boreal forest. *The ISME Journal* **12**: 2187–2197.

Sulman BN, Shevliakova E, Brzostek ER, Kivlin SN, Malyshev S, Menge DNL, Zhang X. **2019**. Diverse Mycorrhizal Associations Enhance Terrestrial C Storage in a Global Model. *Global Biogeochemical Cycles* **33**: 501–523.

Sützl L, Laurent CVFP, Abrera AT, Schütz G, Ludwig R, Haltrich D. **2018**. Multiplicity of enzymatic functions in the CAZy AA3 family. *Applied Microbiology and Biotechnology* **102**: 2477–2492.

Taylor AFS, Martin F, Read DJ. **2000**. Fungal Diversity in Ectomycorrhizal Communities of Norway Spruce [*Picea abies* (L.) Karst.] and Beech (*Fagus sylvatic*a L.) Along North-South Transects in Europe. In: Schulze E-D, ed. Ecological Studies. Carbon and Nitrogen Cycling in European Forest Ecosystems. Berlin, Heidelberg: Springer, 343–365.

Tedersoo L, Smith ME. **2013**. Lineages of ectomycorrhizal fungi revisited: Foraging strategies and novel lineages revealed by sequences from belowground. *Fungal Biology Reviews* **27**: 83–99.

Terrer C, Phillips RP, Hungate BA, Rosende J, Pett-Ridge J, Craig ME, van Groenigen KJ, Keenan TF, Sulman BN, Stocker BD, *et al.* 2021. A trade-off between plant and soil carbon storage under elevated CO_2. *Nature* **591**: 599–603.

Terrer C, Vicca S, Hungate BA, Phillips RP, Prentice IC. **2016**. Mycorrhizal association as a primary control of the CO_2 fertilization effect. *Science* **353**: 72–74.

Toljander JF, Eberhardt U, Toljander YK, Paul LR, Taylor AFS. **2006**. Species composition of an ectomycorrhizal fungal community along a local nutrient gradient in a boreal forest. *New Phytologist* **170**: 873–884.

Treiber ML, Taft DH, Korf I, Mills DA, Lemay DG. **2020**. Pre- and post-sequencing recommendations for functional annotation of human fecal metagenomes. *BMC Bioinformatics* **21**: 74.

Villares A, Moreau C, Bennati-Granier C, Garajova S, Foucat L, Falourd X, Saake B, Berrin J-G, Cathala B. **2017**. Lytic polysaccharide monooxygenases disrupt the cellulose fibers structure. *Scientific Reports* **7**: 40262.

Violle C, Navas M-L, Vile D, Kazakou E, Fortunel C, Hummel I, Garnier E. **2007**. Let the concept of trait be functional! *Oikos* **116**: 882–892.

Vitousek PM, Howarth RW. **1991**. Nitrogen limitation on land and in the sea: How can it occur? *Biogeochemistry* **13**: 87–115.

Wasyliw J, Karst J. Shifts in ectomycorrhizal exploration types parallel leaf and fine root area with forest age. *Journal of Ecology* **108:** 2270-2282

Wood DE, Lu J, Langmead B. **2019**. Improved metagenomic analysis with Kraken 2. *Genome Biology* **20**: 257.

Zak DR, Argiroff WA, Freedman ZB, Upchurch RA, Entwistle EM, Romanowicz KJ. **2019a**. Anthropogenic N deposition, fungal gene expression, and an increasing soil carbon sink in the Northern Hemisphere. *Ecology* **100**: e02804.

Zak DR, Pellitier PT, Argiroff W, Castillo B, James TY, Nave LE, Averill C, Beidler KV, Bhatnagar J, Blesh J, *et al.* 2019b. Exploring the role of ectomycorrhizal fungi in soil carbon dynamics. *New Phytologist* **223**: 33–39.

Zak DR, Pregitzer KS. **1990**. Spatial and Temporal Variability of Nitrogen Cycling in Northern Lower Michigan. *Forest Science* **36**: 367–380.

Zak DR, Pregitzer KS, Host GE. **1986**. Landscape variation in nitrogen mineralization and nitrification. *Canadian Journal of Forest Research* **16**: 1258–1263.

Zanne AE, Abarenkov K, Afkhami ME, Aguilar-Trigueros CA, Bates S, Bhatnagar JM, Busby PE, Christian N, Cornwell WK, Crowther TW, *et al.* 2020. Fungal functional ecology: bringing a trait-based approach to plant-associated fungi. *Biological Reviews* **99:** 409-433

Figure 1: A). NMDS plot of ectomycorrhizal (ECM) fungal communities (points) inhabiting *Quercus rubra* root tips colored by rates of net N mineralization (μgN • g soil^{-1} • day $^{-1}$; legend bar). The vectors indicate degree of correlation between the NMDS axes and hyphal morphologies. Medium and Short indicate hyphal exploration types and Contact and Rhizomorphic indicate presence of rhizomorphic hyphae. Plotted genus names represent scaled centroids for dominant (indicator) ECM fungal genera. B). TITAN analysis depicting indicator ECM fungal genera. Peak along the soil gradient (x-axis) represents location of greatest shift in generic relative abundance. ECM fungal genera that responded negatively s(green), or positively (blue) to rates of net N mineralization. Double peaks represent asynchronous shifts in community abundance, likely due to different underlying species responses.

Figure 2. Generalized dissimilarity model (GDM) output depicting significant predictors (panels) of shifts in ectomycorrhizal (ECM) fungal community composition (A,B,C) and metagenomic decay potential attributed to ECM fungal communities (D,E,F). The slope and shape of the line depict the rate of compositional change along the standardized gradient (x-axis). The maximum height of the regression line (on the y-axis) indicates the relative proportion of variance explained by each standardized variable. ECM fungal communities were sampled from *Quercus rubra* root tips.

Figure 3: Fungal gene families targeting major substrates that form SOM. Points represent the summed abundance of fungal genes targeting individual substrates (panels). A. Cellulose (t = -1.37, *P* = 0.18); B. Hemicellulose (t = 1.00, *P* = 0.32); C. Lignin (t = -1.22, *P* = 0.23); D. Chitin (t = -1.03, *P* = 0. 31), red trend lines represent model fit taking into account geographic sampling structure. Note distinct y-axis scales. Fungal genes and relationships underlying substrate responses are presented in the Supplementary Methods. Fungal decay genes are primarily attributed to ectomycorrhizal (ECM) fungal communities, which were sampled from *Quercus rubra* root tips.

Figure 4: Fungal gene families encoding different enzymes (panel headings: A.,B.,C.) mediating SOM decay. Lines represent model fit accounting for geographic spatial sampling structure. AA2 is presented for clarity, demonstrating role of distinct gene databases. Fungal decay genes are primarily attributed to ectomycorrhizal (ECM) fungal communities, which were sampled from *Quercus rubra* root tips.

Figure 5. A). The abundance of fungal decay genes predominately exhibits negative responses to increasing rates of net N mineralization. Gene families were identified as positive (n=20) and negative (n=15) indicators and summed. Trend lines represent statistical model fits that incorporates geographic sampling structure B). TITAN analysis depicts 'indicator' gene families. Peak along the soil gradient (x-axis) depicts location of greatest shift in gene relative abundance. Green indicates genes that responded negatively (green) or positively (blue) to rates of net N mineralization. Fungal decay genes are primarily attributed to ectomycorrhizal (ECM) fungal communities, which were sampled from *Quercus rubra* root tips.

Figure 6. Relative abundance of ectomycorrhizal (ECM) fungal hyphal foraging types (colors) and the log-transformed abundance of fungal gene families (n=15) that exhibited consistently

negative responses (indicator gene families) to rates of net N mineralization (rhizomorphic T= 1.39, *P*= 0.17; spatial LME) (medium distance exploration types; T = 1.66, *P* = 0.10; spatial LME). Colored bands denote standard error confidence intervals. Fungal decay genes are primarily attributed to ectomycorrhizal (ECM) fungal communities, which were sampled from *Quercus rubra* root tips.

Figure 7. The relative abundance of the ectomycorrhizal (ECM) fungus *Cortinarius* is positively correlated with the log-transformed abundance of Manganese-peroxidase (MnP) genes. MnP genes were normalized to the total number of putative fungal genomes present in each sample; *P* = 0.13 linear model shown in red line with standard error shaded band. Linear mixed model accounting for potential spatial autocorrelation (*P* = 0.37). Fungal decay genes are primarily attributed to ectomycorrhizal (ECM) fungal communities, which were sampled from *Quercus rubra* root tips.

The following Supporting Information is available for this article:

Fig. S1 Map of study sites

Fig. S2 Mineralization rates over the course of the growing season

Fig. S3 Colonized root-tips across the soil mineralization gradient

Fig. S4 Freeze-dried weight of root-tips collected across the soil mineralization gradient

Fig. S5 Alpha diversity of ectomycorrhizal communities

Fig. S6 Metagenomic sequencing yield

Fig. S7 Single copy gene counts per million metagenomic sequences

Fig. S8 Abundance of fungal genomes estimated using metagenomic sequencing

Fig. S9 Change points for negatively responding gene families to soil carbon availability

Fig. S10 Change points for gene families responding positively to soil water availability

Fig. S11 Change points for gene families responding negatively to soil water availability

Fig. S12 Non-ECM fungi present in each sample

Fig. S13 GDM with non-ECM fungi as predictor

Table S1 CAZy gene families, enzymes and substrates

Table S2 Generalized dissimilarity model (GDM) output

Table S3 Metagenomic sequence yield

Table S4 Mixed model output of gene family responses to soil mineralization rates

Methods S1 Detailed sampling and bioinformatic protocols

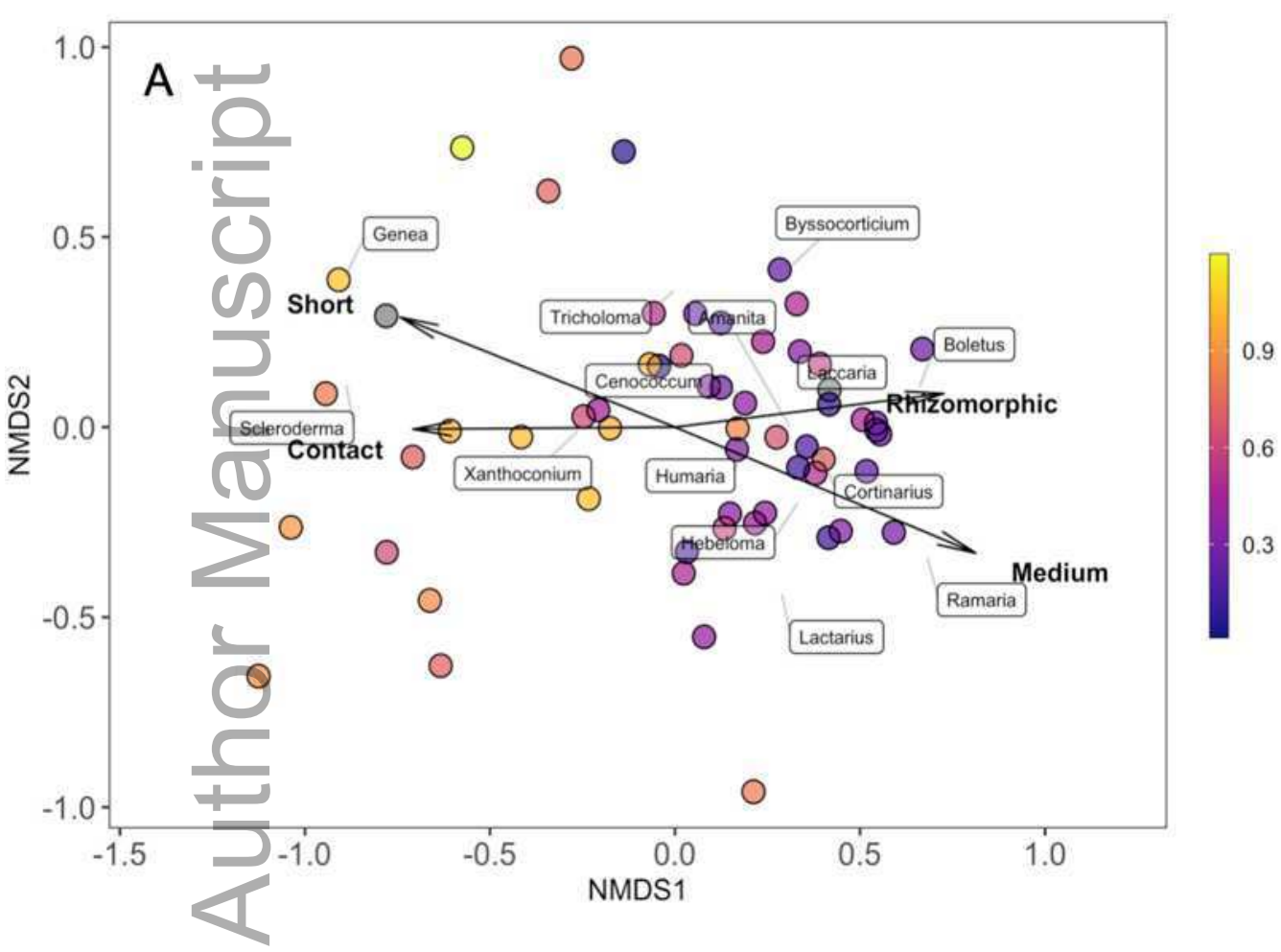

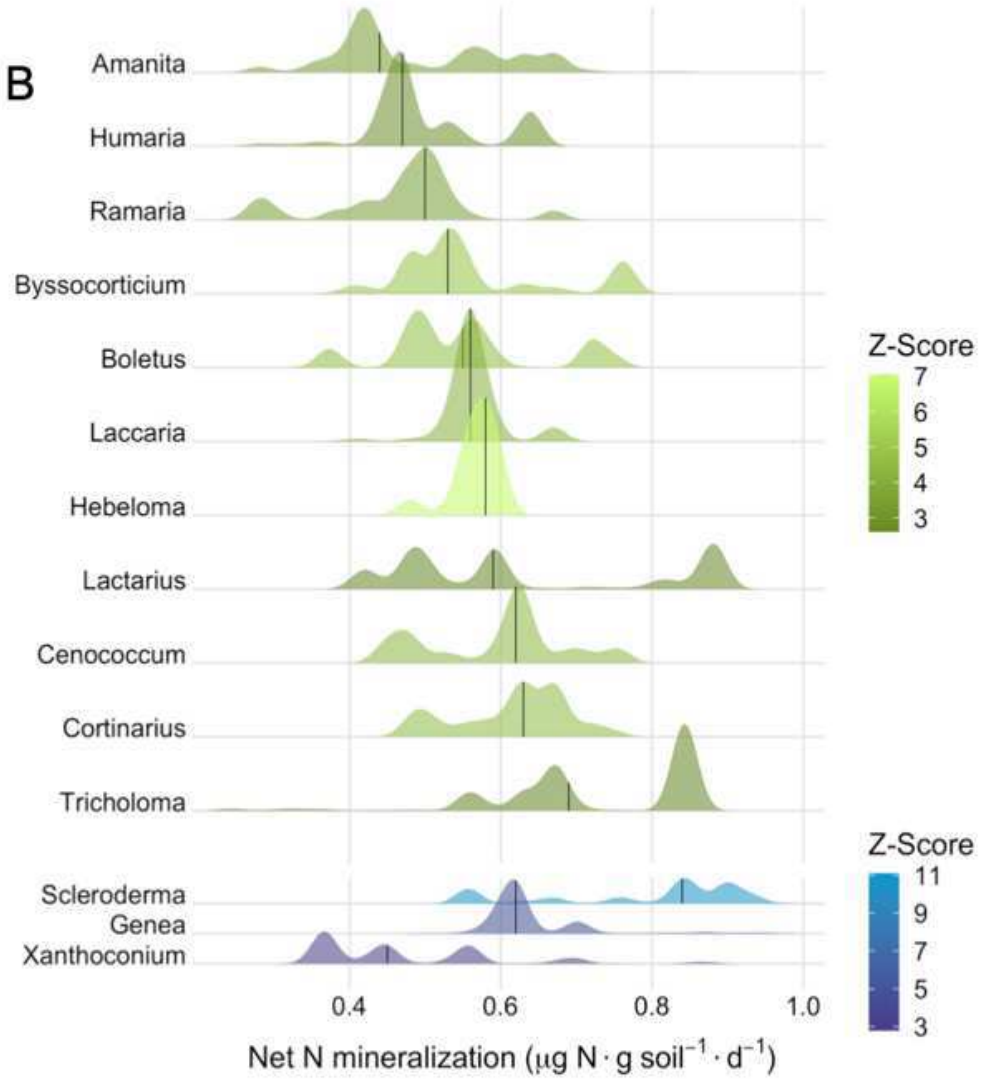

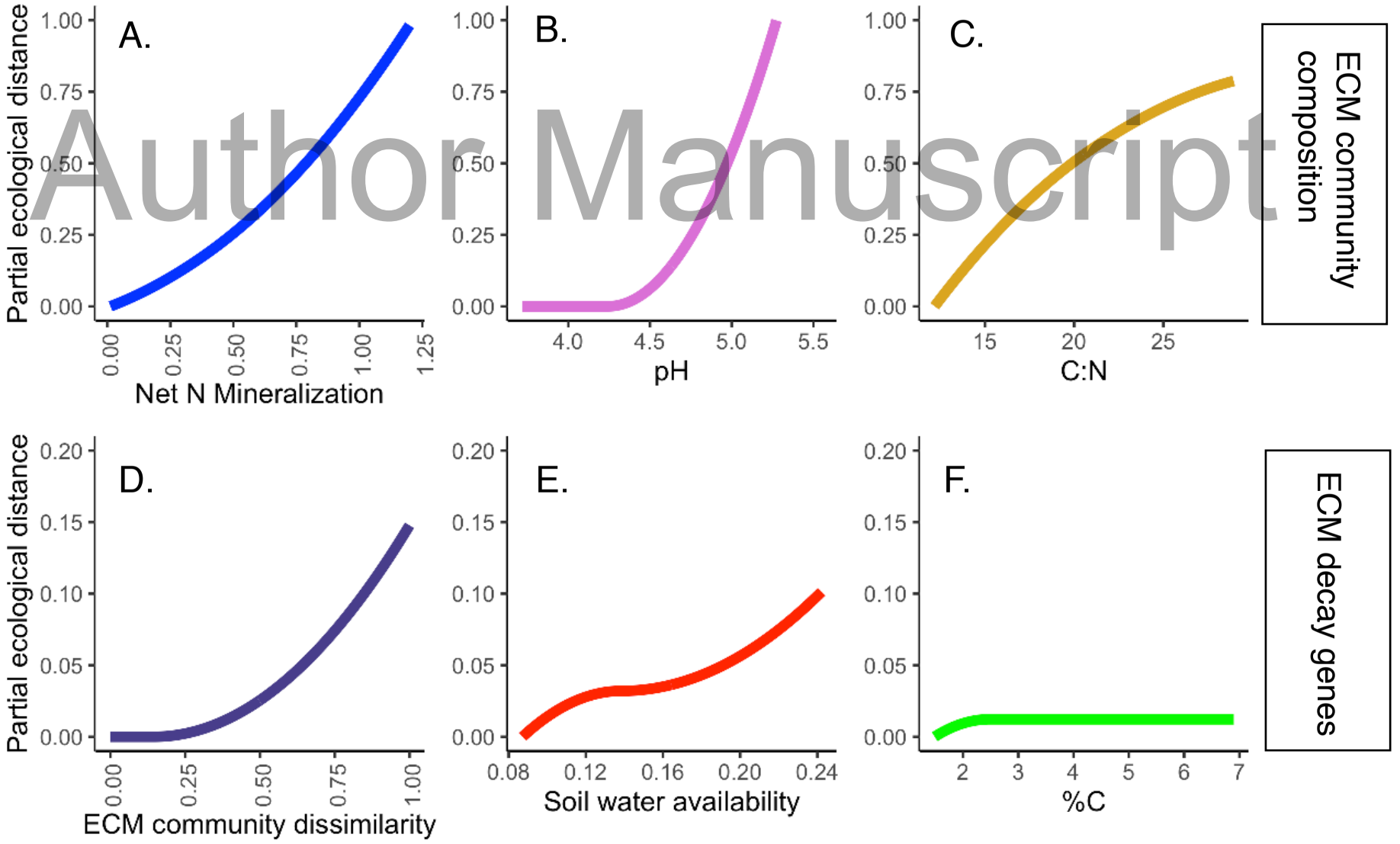

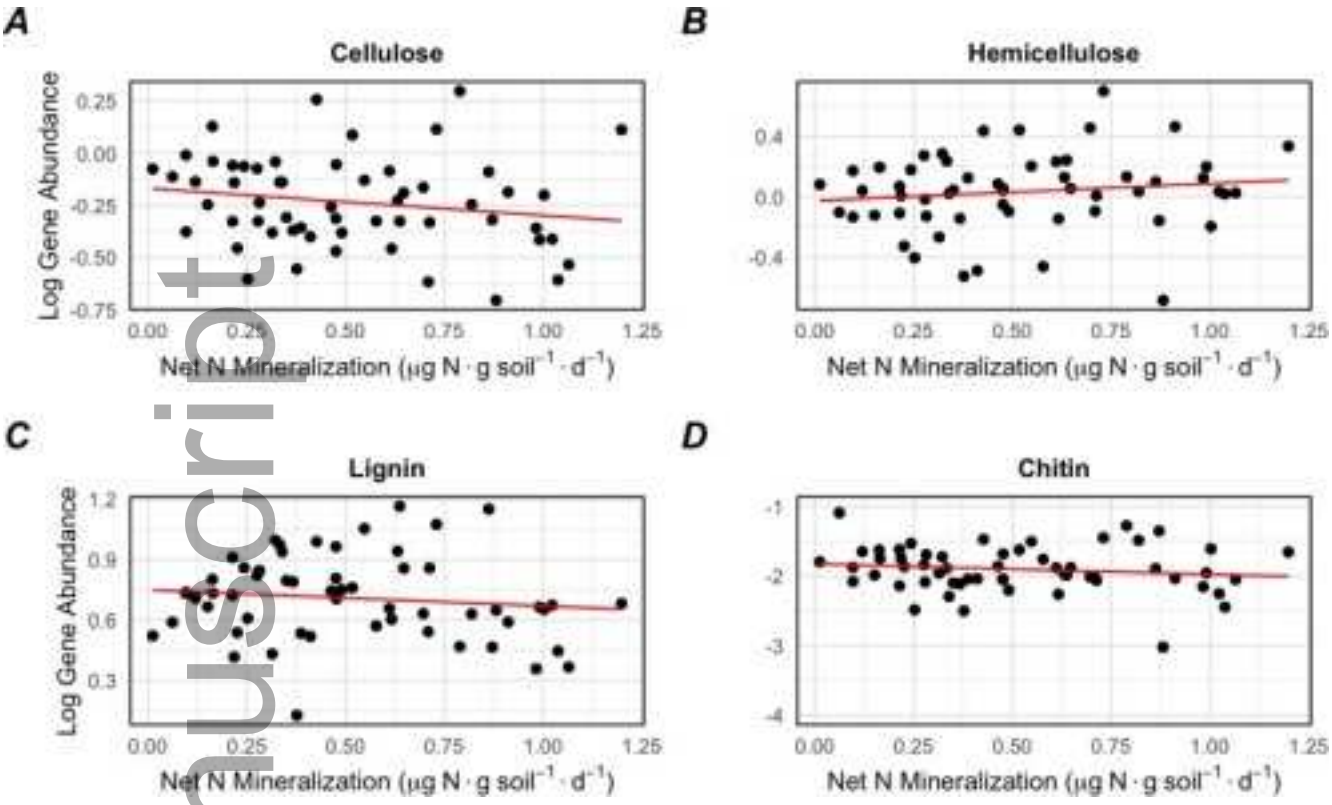

nph_17734_f3.png

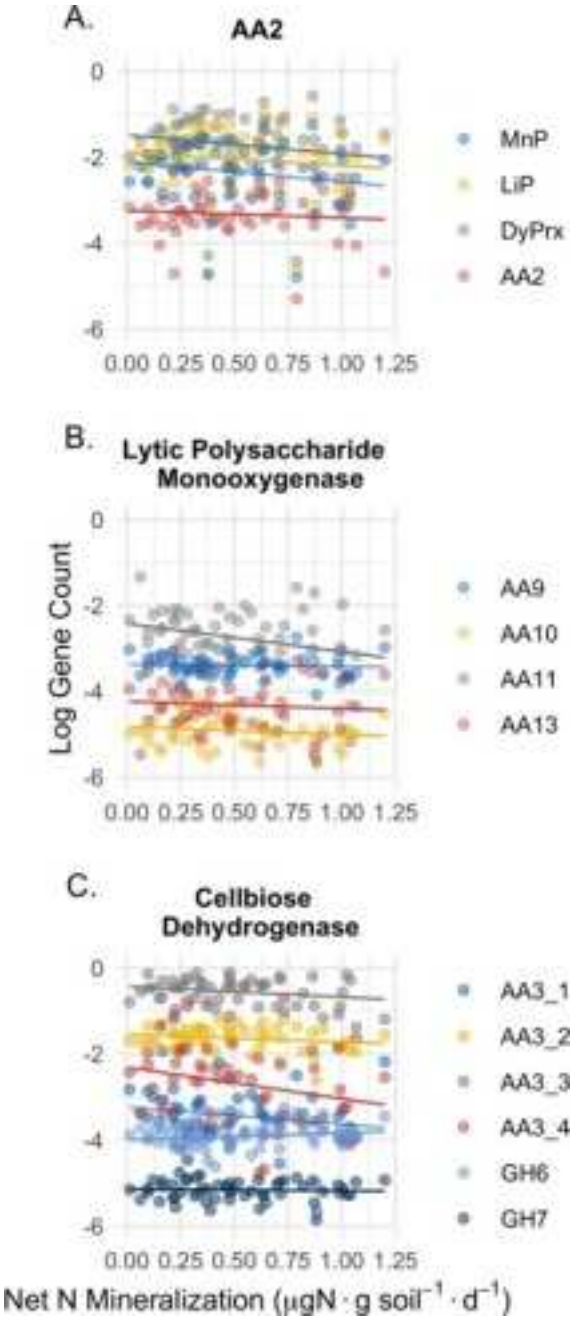

nph_17734_f4.png

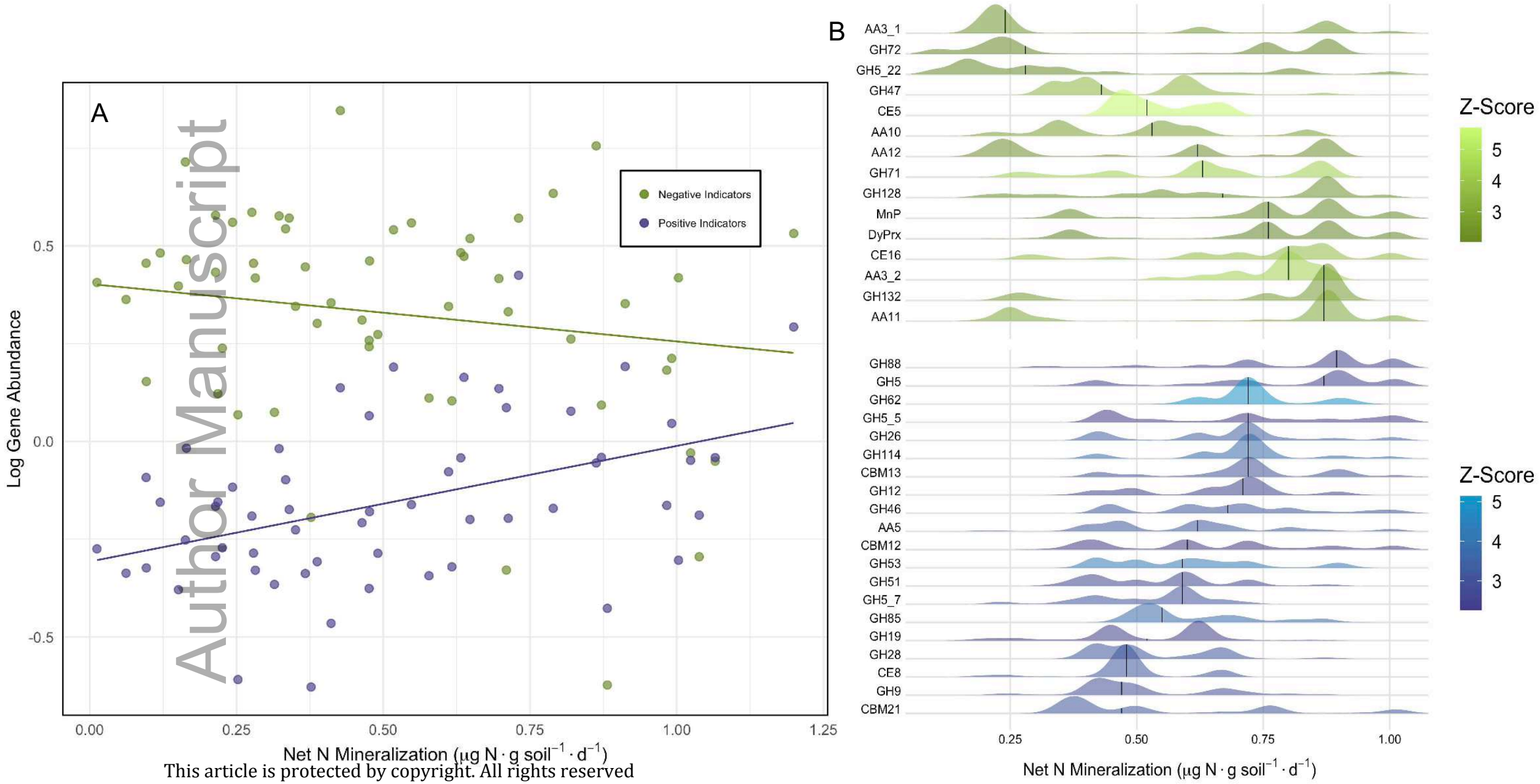

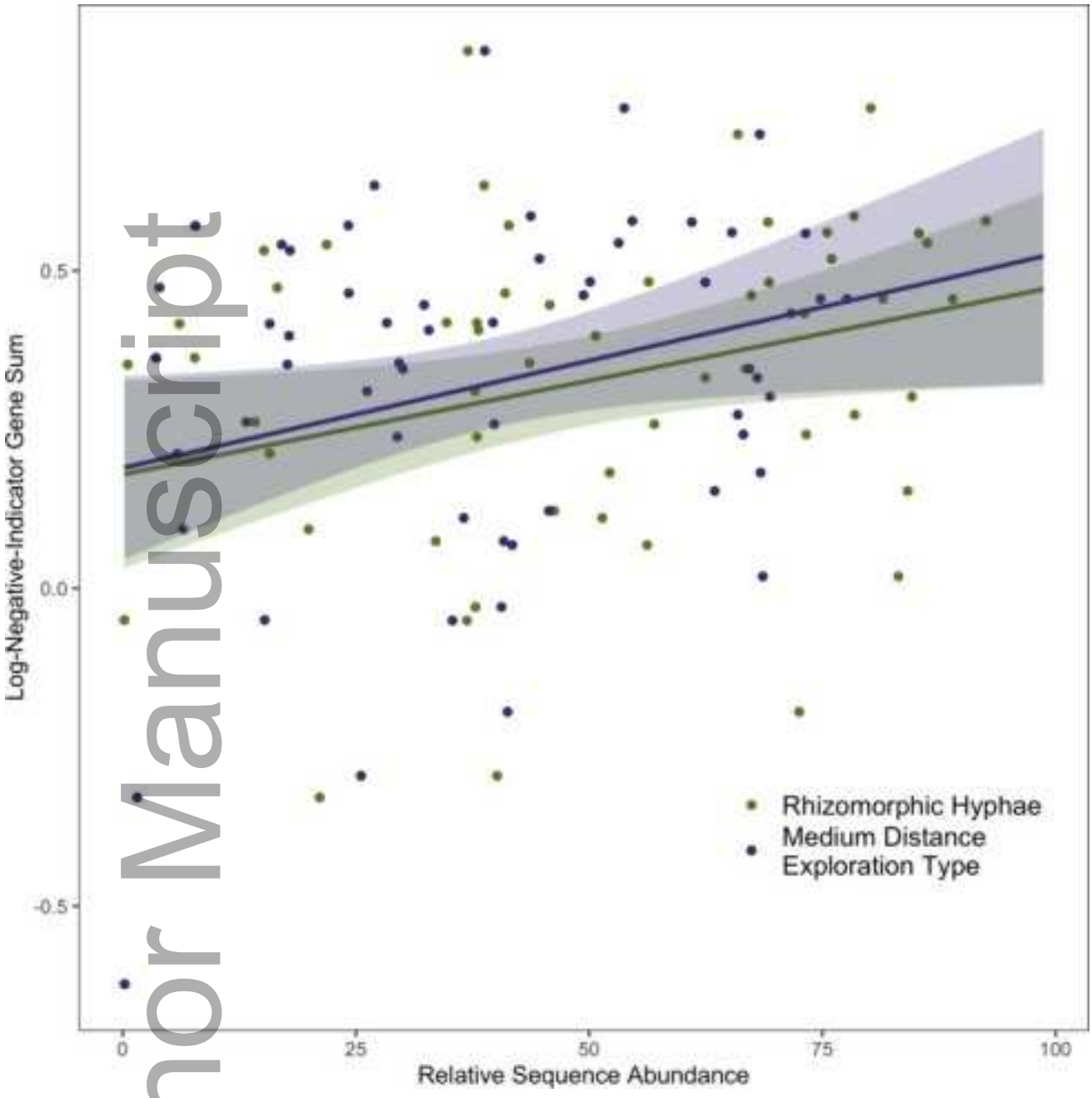

nph_17734_f6.png